

Complex Formation Through Heterogeneous Nucleation of Thermoreversible Gelation

Jean-Michel Guenet*, Daniel Lopez

Laboratoire de Dynamique des Fluides Complexes, Université Louis Pasteur-

CNRS UMR 7506, 4, rue Blaise Pascal, 67070 STRASBOURG Cedex FRANCE

SUMMARY: The preparation method and the molecular structure of a composite material consisting of a ternary system *polymer/bicoppercomplex/solvent* are presented. The properties of each binary system are exposed first. The *polymer solutions* produce thermoreversible gels while the *bicopper organic complex* forms a randomly-dispersed, self-assembling structure in organic solvents. It is shown that, in a common solvent, the *bicopper complex* acts as a nucleation agent for the gelation of the polymer (heterogeneous nucleation). As a result, bicopper complex filaments are encapsulated in a polymer matrix.

Introduction

The occurrence of high- T_c superconductivity in exotic materials such as YBaCuO, a rare earth compound¹ or fullerenes² has prompted the quest for other types of materials liable to exhibit this property. This is the more so as the origin of superconductivity in these materials is still poorly-understood. In the case of YBaCuO, the two-dimensional arrangements of the copper oxide seems to play a major role. Clearly, materials containing copper oxide arrangements are of interest as they may allow one to cast some light on this phenomenon.

The results presented in this paper show how a one-dimensional arrangements of copper oxide structures can be obtained by encapsulating a self-assembling bicopper complex in a polymer matrix. This is achieved by taking advantage of the heterogenous nucleation effect in the case of thermoreversible gels from isotactic polystyrene: *the filaments of bicopper complex act as nucleating agent for the polymer*, and as a result are encapsulated by polymer chains. We shall first describe the binary systems: the polymer system (isotactic polystyrene thermoreversible gels prepared in *trans*-decalin), and the self-assembling bicopper complex (also in *trans*-decalin). Finally, we shall present the preparation conditions and the nanostructure of the resulting material.

Thermoreversible gelation of isotactic polystyrene

Isotactic polystyrene (iPS) thermoreversible gels display a fibrillar morphology whose mesh size is typically of the order of 0.1-1 μm for moderately-concentrated solutions (5-10%). The fibrils show cross-section polydispersity with cross-section radii located somewhere between 2-20 nm^3 . Unlike agarose gels, fibrils are not straight but display a significant amount of distortion. This can be expressed through a parameter, the fractal dimension of the fibril long axis D_f (longitudinal fractal dimension). Further details on this approach will be given below. Isotactic polystyrene produces gels in large variety of solvents^{3,4,5}, of which *trans*- and *cis*-decalin. These two solvents differ only slightly at the level of their conformation (*boat*-conformation for *cis* and *chair*-conformation for *trans*), and yet they produce gels of markedly differing properties⁵.

The temperature-concentration phase diagrams reveal the existence of polymer-solvent compounds⁶. These compounds do not possess the same stoichiometry: 1.75 *cis*-decalin molecule/monomer against 1.15 *trans*-decalin molecule/monomer. The gel is therefore a biphasic system where the polymer-rich phase is more or less organized with inclusion of solvent molecules.

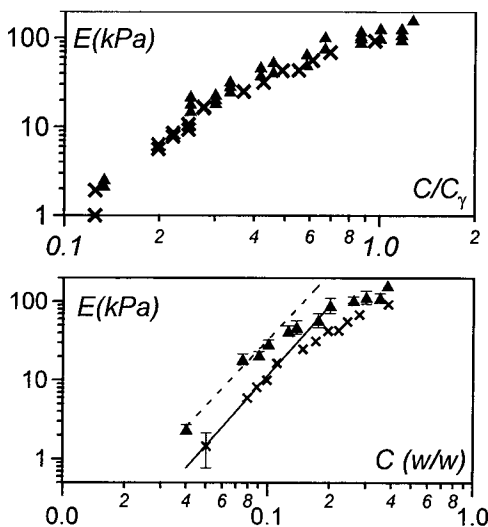


Fig. 1: lower figure: isochronous elastic modulii as a function of polymer concentration as determined by McKenna and Guenet⁷. Upper the same values replotted as a function of C/C_γ , where C_γ is the stoichiometric concentration. \circ = *cis*-decalin; \diamond = *trans*-decalin

The values of the stoichiometry can be used to cast some light on the mechanical properties, particularly for the relation between the elastic modulus and the concentration. As can be seen in figure 1 (lower) values of the elastic modulus found for isotactic polystyrene gels in *cis*-decalin are about three times larger than those in *trans*-decalin. If only the solvent quality were to take into account then there should not be any noticeable difference as the θ -temperature determined with atactic polystyrene for the two solvents is close enough⁸. To account for the difference between either isomers one has to consider the notion of polymer-solvent compounds of different stoichiometries. ***The relevant parameter is the volume fraction of the phase responsible for the elastic properties***, i.e. the polymer-rich phase. Assuming that the polymer concentration of the polymer-poor phase is low enough, then the fraction of polymer-rich phase is obtained by rescaling the polymer volume fraction by the stoichiometric polymer volume fraction ($\phi/\phi_\gamma \sim C/C_\gamma$). A plot of the elastic modulus E vs C/C_γ reveals an universal behaviour (figure 1, upper), which suggests a similar mesoscopic morphology for both systems. Incidentally, the exponent of the initial power law behaviour

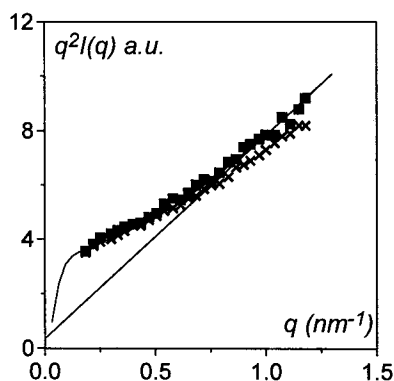


Fig.2: Neutron scattering data⁴ plotted by means of a Kratky-plot ($q^2 I(q)$ vs q). Only a small fraction of chains are labelled so that the single chain behaviour can be obtained. iPS/*cis*-decalin $C = 0.15$ g/cm³. (◊) = gel state, (●) = molten gel state at 66°C. Straight line = asymptote for $ql_p > 1$, full line = theoretical line using Yoshisaki and Yamakawa's relation with $l_p \approx 4$ nm.

($E \sim C^{2.9 \pm 0.2}$) can be analyzed in the framework of Jones and Marques theory⁹. It yields a longitudinal fractal dimension $D_F \approx 1.44$ which is consistent with morphological observations, i.e. distorted fibrils.

The determination of the *chain conformation* in these gels allows one to throw some light on the reason why compounds are formed and on the origin of the poor molecular organisation of

the polymer-rich phase. This study has been performed by small-angle neutron scattering by labelling a small fraction of isotactic polystyrene chains¹⁰. The results are drawn in figure 2.

The scattering curve obtained for the single chain behaviour in the gel state can be accounted for by considering a *worm-like chain*. A worm-like chain is characterized by a persistence length l_p ¹¹. Below l_p the chain is rod-like, i.e. rigid, while above l_p the chain is brownian (gaussian-like). For an infinitely-long chain of mass per unit length μ_L the scattering curve shows two asymptotes¹²:

$$\text{for } ql_p < 1 \quad I(q) \propto 6\mu_L / l_p \quad 1.a$$

$$\text{for } ql_p > 1 \quad q^2 I(q) \propto \pi\mu_L q + 2\mu_L / 3l_p \quad 1.b$$

In the case of finitely-sized chain (with a contour length L), the first asymptotic behaviour is not seen. Instead one must use a semi-empirical relation derived by Yoshisaki and Yamakawa¹³. This gives the theoretical curve on figure 2 from which one derives $l_p \approx 4 \text{ nm}$, i.e. a persistence length 4 times larger than that in the usual flexible state.

This type of chain conformation explains why the gel state displays very poor molecular ordering: a bunch of worm-like chains of such persistence length cannot produce very high order. Intuitively speaking, the longer the chain persistence length, the straighter the fibrils produced by a simple bunching process of the chains. For instance, chain persistence length of agarose chains is rather large¹⁴ which is consistent with the fact that agarose gel fibrils are very straight ($D_F \approx 1$). Conversely, iPS chains persistence length is much shorter, and correspondingly, the fibrils are askew with a longitudinal fractal dimension larger than 1.

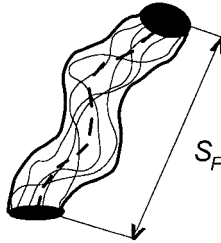


Fig.3: Schematic representation of a fibril made up by bunching worm-like chains together. The dotted line stands for the fibril long axis. It is characterized by a contour length L_F and an end-to-end distance S_F .

That a correlation between chain persistence length and fibril longitudinal fractal dimension exists, can be qualitatively shown from simple arguments. We shall consider a fibril made up by bunching chains of same length. Let L_F be the contour length of the longitudinal axis of

this fibril, and S_F the end-to-end distance. For the sake of simplicity, we shall assume that chain ends are located within the circular ends of the fibril (see figure 3). Chains are assumed to be worm-like and characterized by the same contour length, L and persistence length l_p . The following two relations hold true:

$$S_F^2 \propto N^{2/D_F} a_F^2 \quad 2$$

assuming that the contour length is constituted of N elements of length a_F ,

and:

$$s^2 \propto 2Ll_p \quad 3$$

where s is the chain end-to-end distance. As we assume $s = S_F$ we end up with:

$$l_p / a_F \propto N^{2/D_F} \quad 4$$

which can be rewritten:

$$\text{Log}(l_p / a_F) \propto 2 / D_F \quad 5$$

Relation 5 highlights that the larger l_p the lower D_F , hence the straighter the fibrils and vice-versa.

The other important outcome of the neutron scattering results is the absence of conformational change after gel melting. In usual semi-crystalline polymers the chains retrieve their gaussian, flexible state at crystal melting¹⁵. Here chain stiffness is kept in the sol state thanks to some stabilization mechanism. Guenet had suggested that the chains take on locally a near-3₁ helix stabilized by solvent insertion¹⁶. As a matter of fact, the cavity created by adjacent phenyl rings under the 3₁ form is large enough to house solvent molecules (here it is worth stressing that the solvent molecules are not supposed to fill entirely the cavity but should rather be considered as a prop maintaining the 0.66 nm distance between phenyl rings as they occur in the 3₁ form). Under these conditions rigidity can occur on a sufficient stretch. This view is consistent with the existence of a compound and has received support these past few years^{17,18}.

To summarize, a gel is made up from nanofibrils that are themselves assemblies of worm-like chains. The gel state forms because rigid chains exist in the sol state. As a result, the only way for these chains to organize is to form fibrils. Interestingly, there exist **a well-defined gelation temperature T_{gel}** . Below this gelation temperature a fibrillar gel forms while above spherulitic assemblies grow¹⁹. A gel is not therefore a kinetically-controlled system. Below T_{gel} , in spite of the very slow kinetics, a gel and only a gel will be formed. There is no competition, as

would be expected from a kinetically-controlled process, between gel formation and chain-folded crystal growth. It is, however, worth stressing that cooling a hot solution at an infinitely-slow cooling rate will only produce chain-folded crystals.

The bicopper complex

The bicopper used in this study, portrayed in figure 4, has been synthesized by means of a method devised by P. Maldivi²⁰. It consists of a central core made up with 2 copper atoms surrounded by four oxygen atoms each. On this core are attached aliphatic wings which makes it soluble in a large variety of solvents.

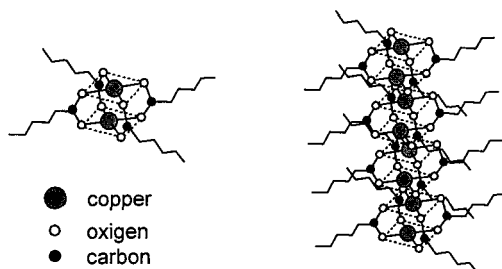


Fig.4: the bicopper complex molecule (left) and the way these molecules pile up to form rigid filaments (right).

In some of these solvents, such as *trans*-decalin, bicopper molecules pile up to form long rigid threads as has been shown by small-angle neutron scattering²¹. As the binding energy between two bicopper complex molecules is of the order of kT , long filaments are characterized by a finite lifetime: brownian motion tend to dismantle them. Meanwhile, other filaments are instantly reformed by a recombination mechanism. These filaments are therefore « *living* » *polymers* according to a terminology used for systems possessing the property to break and reform²².

The rheological behaviour of these « *living* » polymers has been theoretically described by Cates²³. Typically, stress release occurs through two mechanisms: *reptation*, as in usual polymers, and *breaking-recombination* process. Each mechanism possesses its characteristic time (τ_R and τ_b). The characteristic time of the system is then:

$$\tau = (\tau_R \tau_b)^{1/2} \quad 6$$

Two limiting regimes are expected whether τ_R is larger or smaller than τ_b . For $\tau_R < \tau_b$ reptation dominates while for $\tau_R > \tau_b$ the *breaking-recombination* process governs stress relaxation. The solutions of bicopper complex in *trans*-decalin pertain to the latter case. Under these

conditions, the system is described by a near-maxwellian behaviour as far as G' , the storage modulus, and G'' , the loss modulus are concerned. These variables are then written:

$$G' = \frac{G(\omega\tau)^2}{1 + (\omega\tau)^2} \quad 7$$

and

$$G'' = \frac{G(\omega\tau)}{1 + (\omega\tau)^2} \quad 8$$

in which G is the elastic modulus of the plateau regime (for $\omega\tau \gg 1$). Typical characteristic times are close to $1s$.

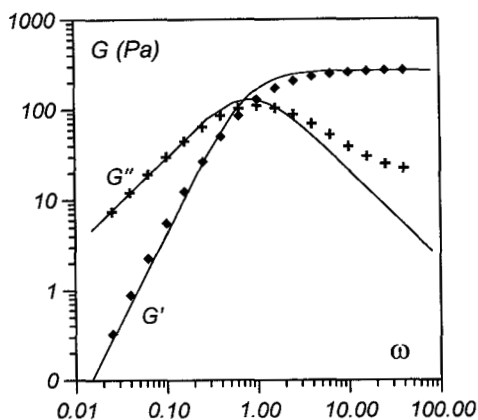


Fig. 5: Typical variations of G' and G'' as a function of frequency for bicopper complex in *trans*-decalin ($C_B = 2\%$ w/w). The solid lines correspond to the best fit with equations 7 and 8. Departure from experimental results for G'' are due to the appearance of other relaxation processes

The lifetime of these filaments is too short to permit solution spinning as required for preparing fibres. As will be shown in the next section encapsulation makes the lifetime infinite. Also, a gel is a better suited medium for preparing macroscopic fibres.

The composite material.

As has been emphasized above, these two systems are prepared in a common solvent, namely *trans*-decalin. At high temperature ($T > 100^\circ\text{C}$) the *bicopper organic complex* no longer forms threads, and turns out to be totally compatible with the polymer. Homogeneous ternary solutions can then be prepared. Interestingly, in this solvent the *bicopper organic complex* starts forming threads well above the gelation threshold of the *polymer*. Typically, threads

longer than 5 to 10 nm are already obtained in the range 70-50°C while $T_{gel} \approx 20^\circ\text{C}$. We therefore wondered whether the bicopper complex could act as a nucleating agent for the gelation process. Indeed, rigid chains may be forced to organize in the presence of long, rod-like filaments.

A DSC study of the evolution of the gelation temperature as a function of the fraction of bicopper complex has been carried out, and is reported in figure 6. It clearly shows an increase of the gelation temperature with some levelling off occurring at a bicopper mole fraction f_c^* . Manifestly, this is the signature of a heterogeneous nucleation process. The fact that both the gel melting temperature and the gel melting enthalpy do not vary with increasing the bicopper mole fraction confirms the heterogeneous nucleation process.

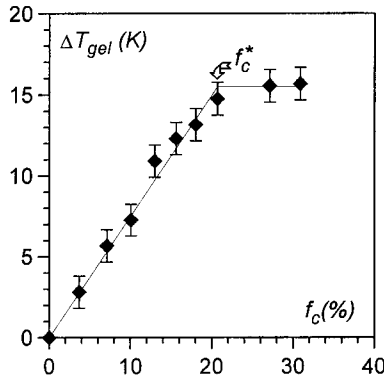


Fig. 6: Increment of the gelation temperature as a function of the bicopper complex mole fraction. $C_p = 0.04 \text{ g/cm}^3$.

The levelling-off corresponds to a phase separation between the bicopper complex and the polymer. Adding more bicopper complex leads to its rejection into a polymer-poor phase. This rejected fraction is obviously of no avail for nucleation purposes.

The nanostructure of the bicopper complex and of the polymer in this ternary system can be studied by small-angle neutron scattering. By using different mixtures of deuterated and hydrogenous *trans*-decalin one can either match the coherent scattering of the hydrogenous complex, which allows study of the deuterated polymer, or match the coherent scattering of the deuterated polymer which allows determination of the hydrogenous bicopper complex structure.

In a high deuterated *trans*-decalin content (91% deuterated/9% hydrogenous in v/v), the nanostructure of the complex is obtained as shown in figure 7. The scattering curves depends upon the mole fraction of bicopper complex. For $f_c = f_c^*$ the scattering curve is very similar

to that obtained in the absence of polymer. It can be fitted with a equation developed for prolate cylinder of lenth L and cross-section r_c for $qL > 1^{25}$:

$$q^2 I(q) \propto C_{Cu} \mu_L \times \frac{4J_1^2(qr_c)}{q^2 r_c^2} \times \left[\pi q - \frac{2}{<L>} \right] \quad 9$$

in which μ_L is the mass per unit length and C_{cu} the bicopper complex concentration, J_1 being the Bessel function of first kind and order 1.

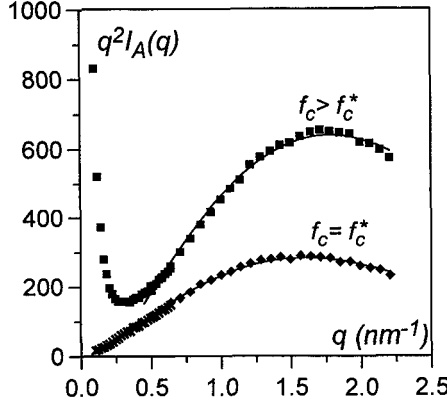


Fig. 7: Scattering curves (Kratky-plot) for $f_c = f_c^*$ (\circ) and $f_c > f_c^*$ (\bullet). The solid lines stand for the best fit using equation 9.

From the fit, one derives $L = 15 \text{ nm}$ and $r_c = 0.8 \text{ nm}$. These data show that the filament structure observed in pure *trans*-decalin is kept. This outcome together with the nucleation effect observed by DSC strongly suggest that bicopper complex filaments are encapsulated in a polymer matrix.

The upturn of the scattering curve at small q -values for $f_c = 2f_c^*$ hints at a two-population system. It can be interpreted with a mixture of monomolecular filaments and three-dimensional objects. The theoretical intensity is then written:

$$q^2 I(q) \propto X \frac{S}{Vq^2} + (1-X) C_H \mu_L \times \frac{4J_1^2(qr_c)}{q^2 r_c^2} \times \left[\pi q - \frac{2}{<L>} \right] \quad 10$$

in which X is the fraction of those three-dimensional crystals, S/V their ratio *surface/volume*. All the other symbols are defined in equation 9.

That two different states for the bicopper complex coexist implies the existence of two phases, a conclusion already reached from the thermodynamic study. Above the critical bicopper complex

fraction f_c^* only a part of the complex efficiently acts as a nucleating agent while the excess is rejected into another phase and eventually forms three-dimensional crystals

In a high hydrogenous *trans*-decalin content (8% deuterated/92% hydrogenous in v/v) the nanostructure of the fibrils of the polymer gel is obtained. In this q -range, the scattering is essentially sensitive to the fibril cross-section.

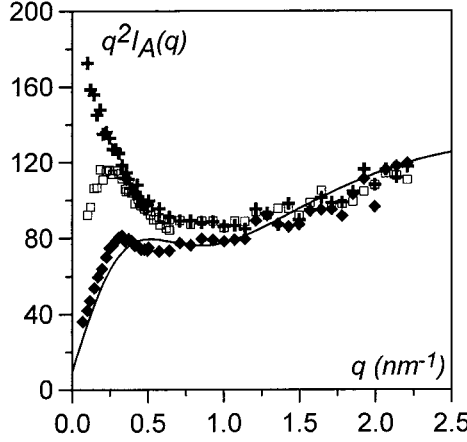


Fig. 8: Scattering curves (Kratky-plot) for iPS gels ($C_{pol} = 0.04 \text{ g/cm}^3$ with differing contents of bicopper complex: (\odot) pure gel; (\diamond) $f_c = f_c^*$; (\triangle) $f_c = 2f_c^*$. The solid line stands for the best fit (see text for details).

In the pure gel state there is a marked upturn at small q -values. In this q -range the scattering curve can be fitted by using a model developed by Guenet²⁶, where fibrils have polydisperse cross-sectional sizes obeying a distribution function $w(r) \sim r^{-\lambda}$ with $0 < \lambda < 3$ bounded by two cut-off radii r_{min} and r_{max} . Typically $r_{min} = 10\text{-}15 \text{ nm}$. The scattering curve at large q -values is close to $I(q) \sim 1/q$, reminiscent of the single chain behaviour. This is due to the existence of the solvation shell that spaces chains from one another. It occurs at $q \approx 1 \text{ nm}^{-1}$ which suggests a spacing of about 1-2 nm.

Upon addition of bicopper complex the upturn gradually vanishes at small q -values. This implies a decrease in cross-section of the fibrils, an effect consistent with the heterogenous nucleation process. In this q -range the scattering curve is best described by:

$$q^2 I(q) = C_p \mu [q f(q\sigma) + z(q)] \approx C_p \mu [q f(q\sigma) + Cte] \quad 11$$

in which σ is some cross-section and μ a mass per unit length. The value of the latter parameter is about $2200 \text{ g/mol} \times \text{nm}$, a value corresponding to 4 chains under a near- 3_1 helical form.

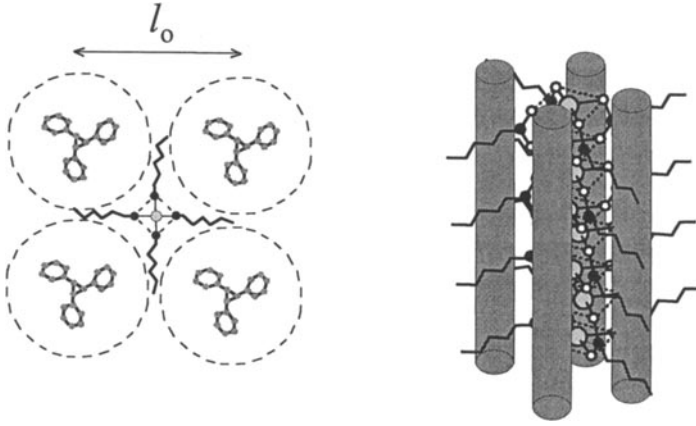


Fig. 9: *left* cross-section of the fibrils of the composite material where polymer chains (grey) under a near-3₁ form encapsulate a bicopper complex filament. The dotted circles stand for the solvation shell. *right* a three-dimensional representation, cylinders stand for the polymer chains.

The model portrayed in figure 9 allows one to account for this scattering curve provided that frozen fluctuations of the distance between chains occur about the most probable value l_o . The following distribution function can be contemplated in order to derive an analytical solution:

$$w(r) = l \exp(-l^2 / 2l_o^2) \quad 12$$

and:

$$q^2 I(q) = \pi \mu_L C_p q \times \frac{4J_1^2(qr_H)}{q^2 r_H^2} \times \left[1 + \exp(-q^2 l_o^2) + 2 \exp(-q^2 l_o^2 / 2) \right] \quad 13$$

in which r_H is the 3₁ helical form radius.

This relation gives the best fit shown in figure 8 with $l_o = 2.4 \text{ nm}$ by taking $r_H = 0.45 \text{ nm}$. This value is consistent with the actual distance l_o expected for these chains keeping in mind the existence of a solvation shell.

Conclusion

Results described here show that a bicopper complex monofilament can be encapsulated by making use of the heterogenous nucleation process. This gives the possibility of preparing macroscopic fibres of nanowires containing one-dimensional arrangement of copper atoms. It now remains to be tested whether this composite material exhibits magnetic properties of interest.

References

- ¹⁾ J.G. Bednorz, K.A. Muller, *Z. Phys.* **B64**, 189 (1986)
- M.K. Wu, et al. *Phys. Rev. Letters* **58**, 908 (1987)
- ²⁾ see for instance M.S. Dresselhaus, G. Dresselhaus, P.C. Eklund *Science of Fullerenes and Carbon Nanotubes*, Academic Press, London (1996)
- ³⁾ J.M. Guenet, B. Lotz, J.C. Wittmann, *Macromolecules* **18**, 420 (1985)
- ⁴⁾ M. Girolamo, A. Keller, K. Miyasaka, N. Overbergh, *J. Polym. Sci., Polym. Phys. Ed.* **14**, 39 (1976)
- ⁵⁾ J.M. Guenet *Thermoreversible Gelation of Polymers and Biopolymers* Academic Press, London (1992)
- ⁶⁾ J.M. Guenet, G.B. McKenna, *Macromolecules* **21**, 1752 (1988)
- ⁷⁾ G.B. McKenna; J.M. Guenet *J. Polym. Sci. Polym. Phys. Ed.* **26**, 267 (1988)
- ⁸⁾ Polymer Handbook, Brandrup and Immergut Ed. (1975)
- ⁹⁾ J.L. Jones, C.M. Marquès, *J. Phys. (Les Ullis)* **51**, 1113 (1990)
- ¹⁰⁾ J.M. Guenet *Macromolecules* **20**, 2874 (1987)
- ¹¹⁾ S. Heine, O. Kratky, G. Porod, J.P. Schmitz *Makromol. Chem.* **44**, 682 (1961)
- ¹²⁾ J. Des Cloiseaux *Macromolecules* **6**, 403 (1973)
- ¹³⁾ T. Yoshisaki and H. Yamakawa *Macromolecules* **13**, 1518 (1980)
- ¹⁴⁾ J.M. Guenet, A. Brûlet, C. Rochas *Int. J. of Biol. Macromol.* **15**, 131 (1993)
- ¹⁵⁾ P.J. Barham, in *Crystallization of Polymers* M. Dosiére Ed. p. 153 (1993)
- ¹⁶⁾ J.M. Guenet *Macromolecules* **19**, 1960 (1986)
- ¹⁷⁾ T. Nakaoki, M. Kobayashi. *J. Mol. Struct.* **242**, 315 (1991)
- ¹⁸⁾ H. Itagaki, I. Takahashi. *Macromolecules* **28**, 5477 (1995)
- ¹⁹⁾ M. Klein, A. Mathis, A. Menelle, J.M. Guenet *Macromolecules* **23**, 4591 (1990)
- ²⁰⁾ P. Maldivi, *Thesis*, Grenoble, France (1989)
- ²¹⁾ P. Terech, P. Maldivi, J.M. Guenet *Europhys. Lett.* **17**, 515 (1992)
- C. Dammer, *Thesis*, Strasbourg, France (1995)
- ²²⁾ G. Porte, J. Appell, Y. Poggi *J. Phys. Chem.* **84**, 3105 (1980)
- ²³⁾ M.E. Cates *Macromolecules* **20**, 2289 (1987)
- ²⁴⁾ D. Lopez, A. Saiani and J.-M. Guenet *Journal of Thermal Analysis* **51**, 841 (1998)
- ²⁵⁾ G. Fournet *Bull. Soc. Franç. Minér. Crist.* **74**, 39 (1951)
- O.A. Pringle, P.W. Schmidt *J. Appl. Crystallogr.* **4**, 290 (1971)
- ²⁶⁾ J.M. Guenet *J. Phys. II* **4**, 1077 (1994)